

## Numerical simulation of macro impact laser peening and the effect of peening on fatigue life and weld residual stresses

Said TAHERI<sup>a</sup>, Emricka JULAN<sup>b</sup>, Eric LORENTZ<sup>a</sup>,

<sup>a</sup>EDF, IMSIA, France, said.taheri@edf.fr eric.lorentz@edf.fr <sup>b</sup>EDF, AMA, France emricka.julan@edf.fr, France

**Keywords:** Laser peening, FEM simulation, fatigue, weld, shot peening

### 1. Introduction

Stress corrosion cracking (SCC) in nickel-based alloy 600 is one of the significant ageing degradations in major components of pressurised water reactors. Components such as steam generator tubes or bottom mounted instrumentation (BMI) in reactor pressure vessels have experienced SCC. Some other components made of austenitic stainless steels subjected to high cycle thermal fluctuations have exhibited thermal fatigue crazing. One common detrimental parameter is frequently the tensile weld residual stress (WRS). Laser peening (LP) is a surface mitigation technique, as is shot peening (SP), for improving the life of metallic components by generating a compressive surface residual stress (RS) field induced by high-power laser pulses. LP has been applied in Japan on several BMI.

Numerical simulations of LP is performed by 3D FEM using a high-speed explicit dynamic code named Europlexus. Numerical validation of Europlexus code for laser peening is performed by comparison of RS obtained by Europlexus and several other codes [1,2]. These RS are also compared with measured RS at stabilised states [1]. However simulated RS did not represent a stabilised state due to considerable CPU times which would be needed to obtain it.

A Johnson-Cook (JC) law is used for all simulations. Parameters of this law for an In600 are identified [3] at a small strain rate  $10^{-3}$  on the stress strain curve, at  $10^3$  to  $5 \cdot 10^3$  by the Hopkinson bar test and at  $10^6$ , which is strain rate of an LP operation, by the VISAR velocimetry technique using laser shock and Doppler effects [4].

In the literature, a characteristic representation of RS after impact is given by the stress plot ( $S_{xx}$  or  $S_{yy}$ , figure 1a) parallel to the impacted surface versus the depth at just one point (this plane is perpendicular to the direction of impact Z). In fact a likelihood assumption under LP or SP operation is that with a large number of impacts the RS field is homogeneous in the X,Y plane (except near the edge of the treated area). The RS field is thus only dependent on the Z coordinate.

Almost total absence of the effect of WRS on RS after LP has been shown in [1] where WRS are approximated by a thermo-visco-plastic simulation. The thermal loading for this simulation is obtained using measured WRS on the surface. In this case however we have no knowledge about the validity of the simulated WRS at depth, so an axisymmetric simulation of welding is performed hier.

Fatigue life may be impacted by strain hardening due to peening, for alloys with memory effects [9]. The beneficial effect of peening on the fatigue life of aluminium alloys (aeronautical industry) and ferritic steel (car industry) has been reported extensively in the literature. However the situation is different for In600 and austenitic stainless steels used in nuclear power plants, as these latter alloys have a memory effect of maximum monotonic (or cyclic) strain hardening. Indeed, it has been shown that [7] for 304 and 316 stainless steel, cyclic pre-hardening of 10 cycles at  $\pm 2\%$  or  $14\%$  monotone strain hardening significantly increases the fatigue lifetime in stress-controlled tests but reduces it in strain-controlled tests (high cycle thermal fatigue). Thus in stress control, the beneficial effect of pre-hardening due to peening is added to the beneficial effect of compressive stress for fatigue life, while in strain control, the detrimental effect of pre-hardening reduces the beneficial effect of compressive stress. Numerical simulations show [8] that SP impacts may create a plastic strain of about 20% while LP creates a plastic strain of about 2%. This may be due to a higher strain rate for LP of  $10^6$  against approximately  $10^5$  for SP. Indeed, in [9] it is shown that, SP has a beneficial effect for 304 stainless steel in strain control at zero mean stress but not at 60 MPa mean stress.

## 2. Objectives

- To show by FEM simulations that the impact of WRS on the final RS obtained after LP is negligible.
- To show by FEM for 2D\_Plane simulations that the plastic strain produced by SP is much higher than the one produced by LP. In the case of SP treatment this plastic strain (strain hardening) cyclically imposed on the metal may have a detrimental effect on fatigue life for alloys with a memory effect (304, 316 stainless steel or In600) [5].
- Previous results must be considered as qualitative, as simulations must be carried out by 3D FEM. However substantial CPU time required to obtain a stabilised RS field by 3D FEM. Thus a reduction in CPU time for LP simulation is obtained by replacing a multiple impact simulation by an equivalent macro-impact simulation. Some validations are presented in this paper.

## 3. Methodology

### 3.1 Impact of WRS before LP on RS after LP:

WRS obtained by an axisymmetric simulation [6] using a coarse mesh is transferred to a more refined mesh for LP simulations (figure 2a). The simulated RS field obtained by LP at depth has been compared in the absence or presence of WRS after 7 superimposed impacts

### 3.2 Effect of strain hardening due to SP or LP on fatigue life for alloys with memory effect

In this paper we show this difference between SP and LP on a numerical simulation by comparing stabilised loops obtained under cyclic loading after peening, since one parameter of fatigue damage is stabilised loop characteristics.

### 3.3 Comparison between macro-impact and multiple impact simulations.

Simulating multiple impact LP in 3D FEM consumes too much CPU time, despite the use of an explicit code (Europlexus [10]). Thus, the RS resulting from the operation of LP prior to SCC calculations is usually obtained by a thermo-elasto-viscoplastic simulation [11]. Nevertheless, an important characteristic of LP is the uniaxial nature of the deformations, which is incompatible with thermo-elasto-viscoplastic modelling. This uniaxial nature is due to a high strain rate of about  $10^6$  which creates an inertial confinement in the direction perpendicular to impact direction (Z), as atoms do not have time to move sufficiently. For the same reason, a 2D\_Plane simulation of RS could not be considered quantitatively valid, as is shown through a comparison with a 3D solution [2]. Consequently, another method is explored here, where the set of mono-impacts on different areas are grouped together in a macro-impact whose spot on the surface is the union of all the mono-impact spots (figure 1b). Moreover the amplitude of the pressure loading represented by a boxcar function of (X,Y) is the same for a mono-impact and for the macro-impact. The analysis carried out here focuses on a plate geometry.

### 3.4 Obtaining a homogeneous field by impacting a restricted area

As mentioned above, a likelihood assumption is that far from the edges of a treated area  $S_{xx}$  and  $S_{yy}$  are homogeneous on the planes perpendicular to the impact direction. The existence of this area therefore suggests the possibility of grouping the different impacts in a single macro-impact. However, to prove the validity of macro-impacting we need to compare stabilised RS obtained by macro-impacting with the one with multiple impacts. It is difficult to make this comparison over the entire treated area (excluding the edge effect) due to the substantial CPU time required. But by applying a sufficiently high number of impacts to a small area it is possible to have access to this homogeneous field in the centre of the area. The comparison will thus be made on this restricted area. It is therefore necessary firstly to ensure the existence of a homogeneous area in the multiple impact case on the treated area. Validation is first performed for unidirectional impact scanning (figure 1a), to obtain the minimum length for the area of the homogenised state of RS. This length is then used for bi-directional scanning, figure 1c.

## 4. Simulation results and analysis

### 4.1 Impact of LP on WRS (axisymmetrical solution)

The simulated RS field obtained by LP at depth has been compared (figure 2a) in the absence or presence of WRS after 7 superposed impacts. Figure 2b shows that WRS has negligible influence on final RS after LP.

### 4.2 Importance of (cyclic) strain hardening due to peening on fatigue life

Figure 3a shows the mesh used for multiple impact SP simulation. The mesh used for multiple impact LP simulation is given in [3]. Figure 3b shows stabilised loops obtained after 20 cycles of uniaxial loading at point A where three cases are compared: a) the surface is not treated; b) the surface is treated by SP; and c) the surface is treated by LP. As may be noticed, the loop without treatment and the one with LP treatment are almost superposed while the loop obtained after SP is larger. When compared to the non-treated case obviously with SP treatment, there is increased fatigue damage due to the cyclic strain hardening component. To run previous simulations it was necessary:

- To make impact simulations with a high strain rate constitutive law such as the JC law;
- To perform the cyclic calculation with a constitutive law with memory-effect such as Chaboche's law [12], where the initial state is induced by LP or SP.

However, since the internal variables differ substantially for both laws, it is not possible to conduct simulations in this way. Accordingly we made chose to carry out the impact simulations and the cyclic simulation under the same Chaboche's law. But as the law is identified at a low strain rate, the induced plastic deformation is greater than with the JC law for impact treatment. Nevertheless, a comparison between the RS obtained by Chaboche's law and by the JC law shows that: the plastic deformation induced by the JC law is respectively 7% and 0.5% for SP and LP while it is 10% and 3% for SP and LP for Chaboche's law. Assuming that the difference between 7% and 10% is minor, we may assume an acceptable calculation for SP. On the other hand, with respect to LP, Chaboche's law gives 3% plastic strain, which considerably overestimates the plastic strain obtained by the JC law (0.5%). Thus the superposition of the loops with and without LP may be assumed to be valid.

### 4.3 Superposed macro-impacts equivalent to a multiple impact

To determine the minimum area on which  $S_{xx}$  and  $S_{yy}$  are homogeneous we use simulations with uni-directional scanning. We will then use the length of this minimum area for bi-directional scanning. RS comparisons are subsequently made between macro-impact and multiple impact for both cases at stabilised states. RS representations are shown on the line AB described on different figures and through the depth at the centre of the area.

**4.3.1 Uni-directional scanning by LP and the homogeneous area:** figure 4 shows  $S_{xx}$  RS parallel to the scan direction on the surface for a multiple impact LP. There are 25 impacts on a length of 10 mm where the impact diameter is 3 mm. This figure proves the existence of the area where the RS is almost homogenised. Nevertheless, there is an oscillation on the RS (about 50 MPa), which is reduced with an increase in the number of impacts and a reduction of the distance between the centres of two successive impacts. In the multiple impact simulation, after 8 series of 25 impacts, RS are stabilised (figure 5a). For macro-impacts we obtained a stabilised state with 14 superposed macro-impacts. It can be noted that there is an area with homogenised RS and the results of the RS obtained by the two methods are very close on this area.

The two peaks at the coordinates of 0.004m and 0.014m are due to an abrupt pressure discontinuity (boxcar functions) at the edge of the treated area. With a Gaussian type load, these peaks would be smaller. Moreover, we see that in 3D simulations these peaks are small and so may be ignored in a simulation by macro-impacts.

Figure 5b shows  $S_{xx}$  RS at depth. The results are very close for the multiple impact and macro-impact cases. It should be noted that the mesh becomes increasingly coarse at depth and therefore both calculations can give differing results at the depth where there is still plasticity.

*4.3.2 Bi-directional scanning by LP and homogenous area:* There is a difference between bi-directional and uni-directional LP. In the bi-directional scanning case, several regular LP sequences may exist. Two examples are given in figure 6. In industrial practice, sequence A is repeated several times (A, A, A, A). But in this case the symmetry with respect to x and y is destroyed. Accordingly a macro-impact which preserves the symmetry (on a plate geometry) will not give the same result as the industrial LP. Accordingly we have also simulated a modified case (A, B, A, B) sequence. We have to simulate several series of 625 superposed impacts ( $25 \times 25$ ). To reduce CPU time, we can reduce the homogenised area to a bare minimum, so in each direction we only take 9 impacts on the same length (10 mm) as for uni-directional scanning.

*Results: sequence (A, A, A, A):* Firstly we performed multiple impact calculations. We achieved stabilisation of the RS field for 4 series of 81 impacts ( $81 \times 4 = 324$  impacts). We have CPU time = 20 hours.  $S_{xx}$  RS on the line AB are plotted as a function of the x coordinate (Figure 7a). For macro-impacts we obtained a quasi-stabilised state for 8 macro-impacts. There is a small homogenised area and the RS results obtained by the two methods are very close. Figure 7b shows the results of RS obtained by multiple impacts and by macro-impacts at depth and also their convergence to a stabilised state. Some differences may be noted: this has to be studied more precisely, but macro-impact RS remains conservative compared to multiple impact RS.

*4.3.3 Comparisons between AAA and ABA, AAAA and ABAB.* Figures 7b and 8 show that RS of ABA and AAA (obtained at the last sequences, so A and A) are perfectly superposed. However, as may be noticed on figure 8, there are non-negligible difference between the RS of AAAA and ABAB (obtained on the last sequences, so A and B).

*4.3.4 Tension zone on the edge of the treated area and comparison between  $S_{xx}$  and  $S_{yy}$ :* Figure 9 shows that  $S_{xx}$  and  $S_{yy}$  are superposed in the centre at the area where the stress fields are homogeneous. However at the edge  $S_{yy}$  which is a principal stress parallel to the edge is in tension while  $S_{xx}$  perpendicular to the edge is not. This tensile stress, however, is smaller than error margin on the RS measures about 50 MPa. It would probably be smaller still if one uses Gaussian pressure instead of a boxcar pressure function.

## Conclusions

- WRS before LP has a negligible effect on RS after LP.
- In contrast with LP, SP may in some cases not be beneficial for fatigue life in strain control for alloys with a memory effect, due to the high plastic strain created.
- For the area where RS perpendicular to the impact direction is homogeneous ( $S_{xx}$ ,  $S_{yy}$ ), the stabilised RS obtained by a multiple impact LP may be approximated by stabilised RS obtained by several superposed macro-impacts. The loading on the macro-impact is the same as on each mono-impact (boxcar function). Moreover the spot of the macro-impact on the surface is the union of the spot of mono-impacts.
- The CPU time is almost the same for macro-impact and mono-impact cases. For a mesh of one million elements, we obtain a stabilised RS state and substantial time savings compared to a multiple impact simulation.
- Multiple impact results show small tensile stresses at the edge for the principal stress component parallel to the edge of the treated area, while this is not the case for the component perpendicular to the edge.

**References**

- [1] E. Julan, S Taheri, C Stolz, P. Peyre, P. Gilles Numerical simulation of laser shock peening in presence of weld for fatigue life design. Proceedings of PVP (28400), 2014, Anaheim, California, USA.
- [2] E. Julan, C. Stolz, S. Tahéri, P. Peyre, P. Gilles : Simulation du traitement de surface par choc laser en présence d'un état initial de contraintes 21ème congrès français de mécanique Bordeaux, (2013).
- [3] E. Julan simulation numérique du choc laser pour la mise en compression en présence de l'état initial dû au soudage. PhD thesis, Ecole polytechnique 2014.
- [4] P. Peyre, L. Berthe, X. Scherpereel, R. Fabbro, and E. Bartnicki Experimental study of laser-driven shock waves in stainless steel J. Appl. Phys. 84, 5985 (1998); doi: 10.1063/1.368894
- [5] S. Taheri S, Hauet A, Taleb L, Crescent K. Micro-macro investigations about the fatigue behavior of pre-hardened 304L steel. Int J Plast (2011;27):1981-2004.
- [6] S. Taheri E. Julan, X-V. Tran, N. Robert Impacts of weld residual stresses and fatigue crack growth threshold on crack arrest under high-cycle thermal fluctuations Nuclear Engineering and Design 311 (2017) 16-27.
- [7] S. Taheri, L. Vincent, J. C. Le-Roux Classification of metallic alloys for fatigue damage accumulation: A conservative model under strain control for 304 stainless steels. Int J of Fatigue 70 (2015) 73-84.
- [8] E. Rouhaud : Modélisation mécanique de la contraction à la mise en compression. Habilitation à diriger les recherches, l'université de Technologie de Troyes.
- [9] S. Taheri, L. Vincent, J. C. Le-Roux A conservative damage accumulation method for the prediction of crack nucleation under variable amplitude loading for austenitic stainless steels. Proceedings of PVP (98274), 2013, Paris, France.
- [10] Europlexus : [http://europlexus.jrc.ec.europa.eu/public/manual\\_pdf/manual.pdf](http://europlexus.jrc.ec.europa.eu/public/manual_pdf/manual.pdf).
- [11] Y. kono, K. okimura, M. tajima, R. Toth, T. Sato C. Jardin, P. Le-Bec Reliability of Water Jet Peening As Residual Stress Improvement. Proceedings of PVP (97405), 2013, Paris, France.
- [12] J. Lemaître and J.L. Chaboche (1996). Mécanique des matériaux solides. Dunod.

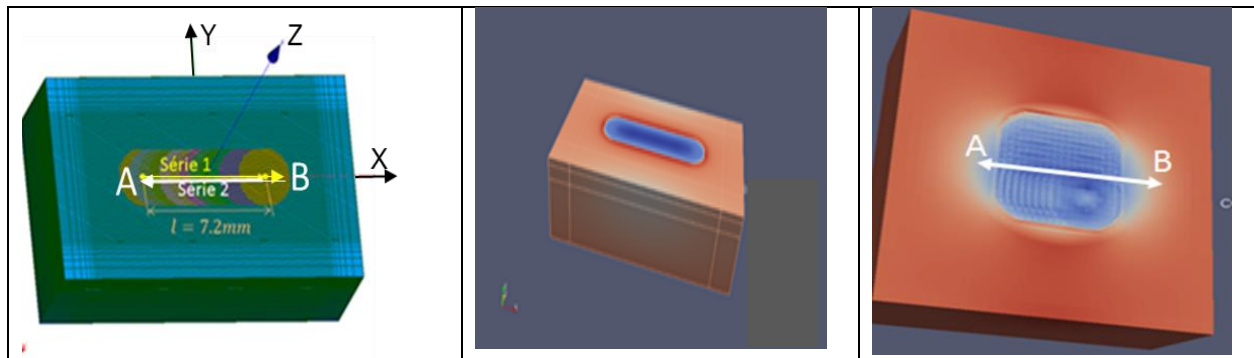


Fig. 1a, LP direction (Z) and the scanning direction (X).

Fig. 1b Macro-impact grouping 25 impacts of figure 1a.

Fig. 1c Two-dimensional LP impacts

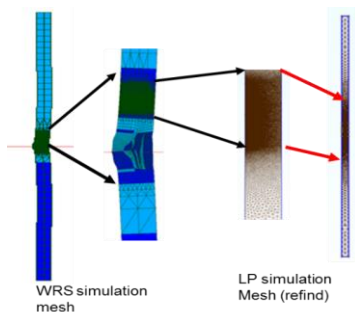


Fig. 2a meshes for WRS and for LP simulations

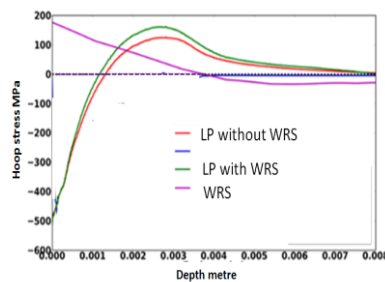


Fig. 2b effect of WRS on final RS after 7 superposed LP

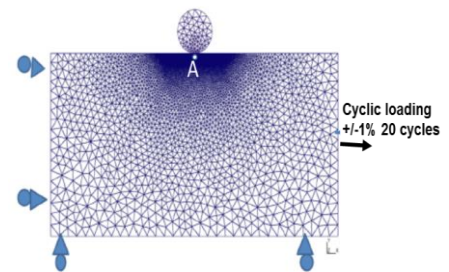


Fig. 3a Mesh for simulation of SP and fatigue analysis

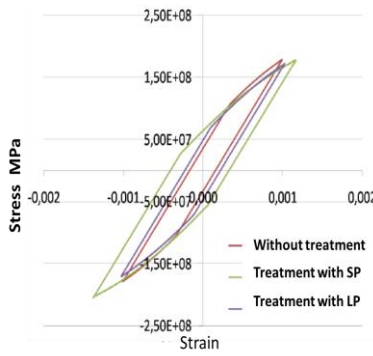


Fig. 3b stabilised loops under cyclic strain control loading (+/-0.1%, 20 cycles) after LP and SP

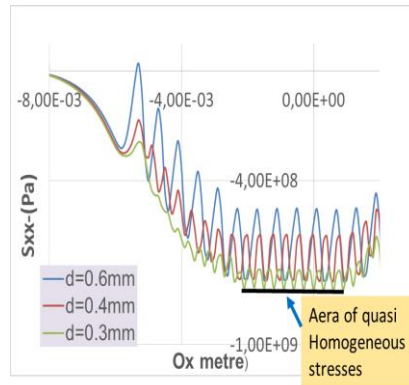


Fig. 4 Sxx RS versus x on the surface. Reduction of RS oscillation with distances between impacts centres

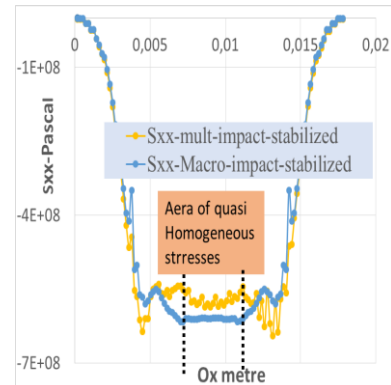


Fig. 5a Sxx RS versus x, and area of quasi-homogeneous RS. Uni-directional scanning

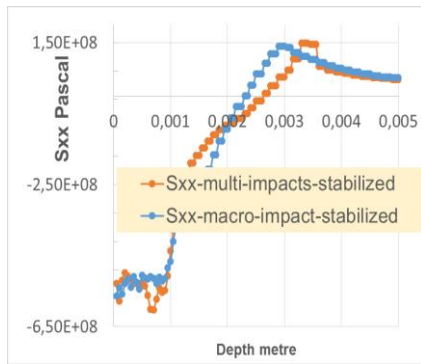


Fig. 5b Sxx RS versus depth. Uni-directional scanning

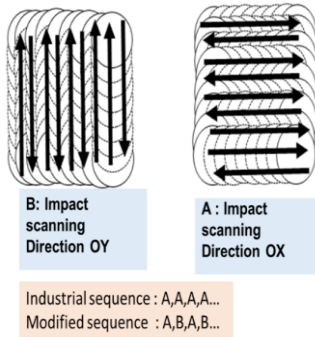


Fig. 6 two regular possibilities in bi-directional scanning

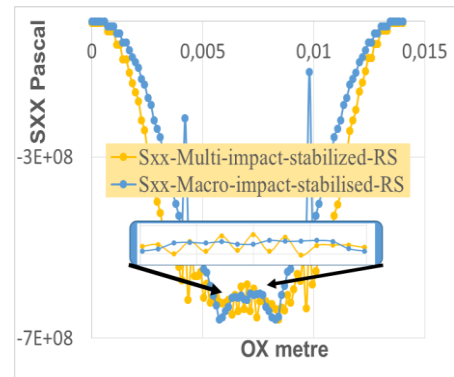


Fig. 7a Stabilised Sx RS for multiple and macro impacts on the surface, AAAA sequence

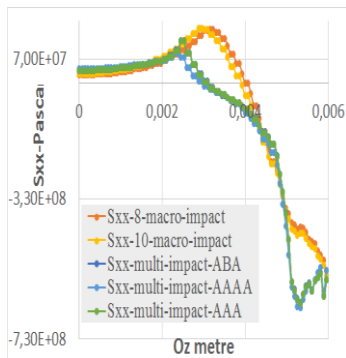


Fig. 7b Multiple impact and macro-impact RS at depth (RS : ABA =AAA)

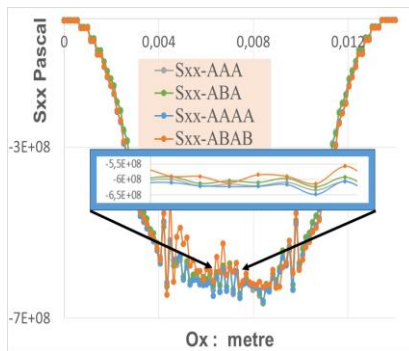


Fig. 8 stabilised Sxx RS on the surface for different sequences

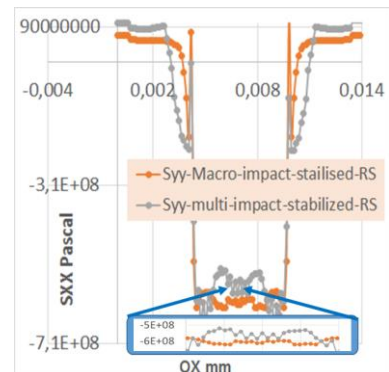


Fig. 9 Tensile stress at the edge for the stress parallel to the edge (Syy)